Epilepsia. Author manuscript; available in PMC 2013 September 10.

Published in final edited form as:
Epilepsia. 2009 December ; 50(12): 2549–2556. doi:10.1111/j.1528-1167.2009.02180.x.

Structures involved at the time of temporal lobe spikes revealed by interindividual group analysis of EEG/fMRI data

Eliane Kobayashi, **Christophe Grova**, **Louise Tyvaert**, **François Dubeau**, and **Jean Gotman**
Montreal Neurological Institute and Hospital, McGill University, Montreal, PQ, Canada

Summary

Purpose—We measured metabolic changes associated with temporal lobe (TL) spikes using combined electroencephalography (EEG) and functional magnetic resonance imaging (fMRI). We selected 18 patients with temporal lobe epilepsy (TLE) who underwent a 2-h simultaneous EEG–fMRI and had unilateral or bilateral independent TL spikes for interindividual group analysis, in order to identify consistent blood oxygenation level dependent (BOLD) responses to TL spikes.

Methods—EEG was postprocessed and spikes were visually identified. fMRI data were preprocessed with motion correction, spatial smoothing, and removal of low frequency drifts. Spike timings were used as events for fMRI statistical analysis. Four hemodynamic response functions were used to account for variability in the BOLD response.

Results—Group analysis revealed common areas of BOLD activations and deactivations. The hemodynamic response function (HRF) peaking 3 s after the spike showed activation involving ipsilaterally the mesial temporal structures (presumably the hippocampus), putamen/globus pallidus, inferior insula, and superior temporal gyrus. The HRF peaking at 5 s showed activations involving ipsi- and contralaterally the superior temporal gyrus and inferior insula. Both HRFs showed bilateral posterior cingulate deactivations.

Discussion—We disclosed involvement of a network of activated areas during unilateral TL spikes, including ipsilateral mesial temporal structures, basal ganglia, and bilateral neocortical temporal regions. Despite the low temporal resolution of fMRI we demonstrated that contralateral temporal involvement occurred later than ipsilateral activation. This contralateral change took place in the absence of visible EEG changes. The posterior cingulate deactivation may reflect the interconnections between this region and other limbic structures. It may also partially correspond to a suspension of the default mode network, as previously described for TL spikes.

Address correspondence to Eliane Kobayashi, MD, PhD, Montreal Neurological Institute and Hospital, McGill University, 3801 University Street, Montreal (PQ), Canada, H3A 2B4. eliane.kobayashi@mcgill.ca.

Disclosure: None of the authors has any conflict of interest to disclose.

We confirm that we have read the Journal's position on issues involved in ethical publication and affirm that this report is consistent with those guidelines.

Supporting Information
Additional supporting information may be found in the online version of this article (http://doi.org/10.1111/j.1528-1167.2009.02180.x)
Please note: Wiley-Blackwell is not responsible for the content or functionality of any supporting information supplied by the authors. Any queries (other than missing material) should be directed to the corresponding author for the article.

Keywords

EEG-fMRI; Temporal lobe epilepsy; Temporal lobe spikes; Group analysis

Temporal lobe epilepsy (TLE) involves primarily mesial temporal structures, but several indicators point to additional involvement of other brain regions (Natsume et al., 2003; Blumenfeld et al., 2004; Bonilha et al., 2004; Ryvlin et al., 2005; Thivard et al., 2005). Temporal lobe (TL) spikes recorded on scalp electroencephalography (EEG) are usually generated in the neocortex, even if they sometimes occur concomitantly with mesial temporal discharges (Ebersole & Wade, 1991; Merlet & Gotman, 1999). Ryvlin and Kahane (2005) introduced the term of “temporal plus epilepsy” to characterize specific forms of multilobar epilepsy with electroclinical features primarily suggestive of TLE. The idea of a spectrum of TL seizures and TLE relates to the possibility that multiple areas are involved in initiation and propagation of epileptic activity, and this would depend on the extent of the epileptic network.

We previously evaluated changes in blood oxygenation level dependent (BOLD) signal to unilateral TL spikes through simultaneous recording of EEG and functional magnetic resonance imaging (EEG–fMRI). In a series of patients with TLE, we observed BOLD responses in the spiking TL, the contralateral homologous cortex, and also extratemporal regions (Kobayashi et al., 2006a). The TLs most frequently displayed bilateral homologous neocortical BOLD responses, and involvement of the mesial temporal regions was much less frequent. The extratemporal responses were not homogeneous across patients, involving various cortical areas and the thalami.

Most EEG–fMRI studies of epileptic patients have been done on individual patients because it is difficult to average a group of subjects that do not have a homogeneous disease. Individual studies result in a much lower signal-to-noise ratio compared to group studies usually performed in neuroscience. If a homogeneous group of patients can be selected, we can disclose involvement of regions that may not be seen in the individual analyses because they do not reach the level of significance required for individual data interpretation, but become visible because they are consistently present among the population. Using group analysis of EEG–fMRI from TLE patients, Laufs and colleagues (2007) identified activation in the hippocampus ipsilateral to the spikes as a common pattern of BOLD response. Involvement of the “default mode network” (i.e., precuneus, posterior cingulate, frontal, and inferior parietal cortices bilaterally, Raichle et al., 2001) as BOLD deactivation was further demonstrated by using a region-of-interest approach. These results suggest a common underlying structure in the BOLD response to TL spikes, which might be important to understand the consequences of the spikes on the epileptic network. In this study, we aimed to identify the underlying common structures involved at the time of a typical TL spike. The evaluation of a larger group of homogeneous TLE patients, without any a priori assumptions in the fMRI analysis, might help us understand what areas are most relevant in the generation of the discharges.

Materials and Methods

Subjects

Eighteen TLE patients with unilateral or bilateral independent TL spikes were selected. The diagnosis of TLE was established according to the International League Against Epilepsy (ILAE) recommendations. We included only patients who had TL spikes restricted to the anterior and inferior temporal electrodes (F7-F8, T3-T4, T5-T6, Zy1-Zy2, F9-F10, and T9-T10). Patients with large structural lesions outside the TLs or with previous surgery were excluded to ensure accurate co-registration in the stereotactic space.

Spikes were classified according to spatial distribution (right or left) and morphology, resulting in two different studies in patients with bilateral independent discharges or in patients with two types of unilateral discharges. Ten patients had a single spike type in the left TL, one had a single spike type in the right TL, and one had two left TL spike types. Six patients had independent left and right TL spikes. This resulted in 25 independent spike types (10 + 1 + 2 + 2 × 6) and thus 25 studies selected for the group analysis (Table S1-online material).

The patients selected for this group study constitute a homogeneous subset of a previous study focusing on individual analysis of EEG–fMRI data from 27 patients (Kobayashi et al., 2006) and five additional patients scanned after this publication. Spike frequency was not a selection criterion, with 4–410 spikes/study (median = 18 spikes/study).

EEG–fMRI acquisition

All patients underwent a 90–120 min recording session. Written informed consent was obtained from each subject, as approved by the Research Ethics Committee of the Montreal Neurological Institute and Hospital. The session started with an anatomic acquisition (1 mm slice thickness, 256 × 256 matrix, TE = 9.2 ms, TR = 22 ms, flip angle 30/), and BOLD fMRI data were collected in runs of 6 min with the patient in the resting state (EPI acquisition, voxel dimensions 5 × 5 × 5 mm, 25 slices, 64 × 64 matrix, TE = 50 ms, TR = 3 s, flip angle 90/), with 9–15 runs/session (average, 11 runs). EEG was continuously recorded inside the MRI scanner (Siemens Sonata, 1.5T) using 21 MRI compatible electrodes (Ag/AgCl) placed on the scalp according to the 10–20 system and additional electrodes covering the inferior temporal regions (F9, T9, P9, F10, T10, P10). Subjects' heads were immobilized with a pillow filled with foam microspheres. Data were transmitted from an EMR32 (Schwarzer, Munich, Germany, 1 KHz sampling rate) or a BrainAmp (Brain Products, Munich, Germany, 5 KHz sampling rate) amplifier via an optic fiber cable to the EEG monitor located outside the scanner room.

Intrasubject data analysis

EEG was postprocessed for offline MRI artifact removal and filtering using the FEMR software (Schwarzer) or Analyzer software (BrainAmp products). An experienced neurophysiologist reviewed filtered EEGs and manually marked the TL spikes.

The functional images were motion corrected and spatially smoothed at 8 mm full width at half maximum (FWHM) using the software package from the Brain Imaging Center of the Montreal Neurological Institute (http://www.bic.mni.mcgill.ca/software/). Runs showing intra-run motion larger than 2 mm or 2 degrees were excluded from the analysis. Models and signals were pre-whitened with an auto-regressive filter of order 1. No physiologic noise correction was performed. However, as advised in Lund et al. (2006), global time courses modeling low frequency drifts and motion parameters were used as confounds in the analysis. Low frequency drifts in the signal were modeled using discrete cosine basis functions ranging from 0 to 0.02 Hz (16 basis functions). Motion parameters obtained after intra-run registration were modeled as confounds using a first-order Volterra expansion (24 regressors).

Maps of the t statistic (t-maps) were created using the timing of each TL spike as an event in the fMRI analysis (fMRIstat software, Worsley et al., 2002). The regressor of interest used to model the BOLD response to TL spikes was the timing of the epileptic events convolved with a hemodynamic response function (HRF). When patients showed two types of independent spikes, two regressors, one for each spike, were generated and included in the design matrix of the general linear model. A t-map for each regressor was subsequently estimated. To take into account some variability in the response to spikes, we used four HRFs consisting of gamma functions peaking at 3, 5, 7 and 9 s after the discharge as described in Bagshaw et al. (2004). For single subject analysis, we usually combine the four t-maps, corresponding to these four analyses in one map by taking the maximum t-value at each voxel. However, intergroup analysis requires the estimation at each voxel of the effect and the standard deviation of the first level analysis (intrapatient), and we have, therefore, looked at the four HRF models independently, which allows us to study variability in the BOLD responses at the group level.

Because some patients may show large amounts of spikes appearing in bursts over specific periods or even during the whole acquisition, some low frequency fluctuations (< 0.02 Hz) may be present in the regressor of interest as well. To avoid degeneracy of the general linear model due to correlations between the regressor of interest and cosines basis functions used to model low frequency drifts, we applied a high-pass filter at 0.02 Hz to the regressor of interest.

The analysis described below was repeated for each HRF. For each subject i, data obtained for each run were first registered and resampled to the position of the first run using a rigid transformation (3 rotations and 3 translations) to correct for possible movement during scanning. No motion exclusion threshold was applied to inter-run co-registration. Statistical results for each run were then averaged using a fixed effects model, leading for subject i to an estimation of the global statistics of the BOLD response E_i, its standard deviation S_i, and the resulting t-statistic $t_i = E_i/S_i$.

Intersubject analysis

The method used for group analysis is basically the same as the method we used in Gotman et al. (2005). The anatomic MRI scans of the 18 patients were spatially normalized in the

stereotactic space of the average brain template from the Montreal Neurological Institute (Collins et al., 1994).

The resulting affine geometrical transformations were used to resample the results of individual fMRI analyses E_i and S_i in the stereotactic space. The spatially normalized images from the studies corresponding to right TL spikes were right–left flipped, such that the hemisphere ipsilateral to all TL discharges will be the left hemisphere in the stereotactic space. The group analysis was performed using a random effects linear model with the effects E_i (as data) and fixed effects standard deviations S_i taken from the analysis of the individual subjects. This model was fitted using restricted maximum likelihood and provided an estimate of the random effects variance (Worsley et al., 2002). As the estimation of random effects variance may be noisy (24 degrees of freedom in this study), we increased the sensitivity of the group analysis using the method proposed by Worsley et al. (2002), which consists in first estimating the ratio of the random effects variance to the fixed effects variance, and then regularizing this ratio by spatial smoothing. The variance is finally estimated by the smoothed ratio multiplied by the fixed effects variance. The amount of smoothing was chosen to achieve 100 effective degrees of freedom. Using such an approach, only the variance ratio is smoothed but not the effects E_i. This group analysis, to which we will refer as a mixed effects group analysis, provided the statistics E, S, and t.

The resulting t statistic images were thresholded using the minimum given by a Bonferroni correction and random field theory, taking into account the non-isotropic spatial correlation of the errors. FWHM maps of the group statistics were first estimated at each voxel from the residuals of the previous analysis. Eight millimeter FWHM smoothing led to a resulting average brain spatial resolution of 16 mm FWHM in the group analysis statistics. The average brain FWHM was used for cluster size test to identify clusters with significant BOLD responses. Voxels considered for this cluster analysis were selected as voxels considered significant at uncorrected $p < 0.005$ located within a mask of the brain. The method then computes the corrected p-value of the spatial extent of each cluster, taking into account the estimated average FWHM in the brain. Every cluster showing a corrected $p < 0.05$ for its spatial extent was considered significant.

Results

According to the intrarun motion selection criterion, only three runs of 10 for one patient only were excluded from the analysis. Significant BOLD responses are summarized in Table 1. For each HRF, cluster volumes, corrected p-value for their spatial extent, and max t-values within each cluster are shown. No significant clusters were found for HRFs peaking at 7 and 9 s.

Results obtained with the HRF peaking 3 s after TL spikes are presented in Fig. 1 and Table 1. BOLD activations were found ipsilaterally in the mesial temporal structures including the hippocampus, the putamen/globus pallidus, the inferior insula, and the superior temporal gyrus (cluster #1, Table 1). BOLD deactivation was found in bilateral posterior cingulate regions (cluster #2, Table 1).

Results obtained with the HRF peaking 5 s after TL spikes are presented in Fig. 2 and Table 1. BOLD activations were found bilaterally (clusters #3 and #4, Table 1) in the superior temporal gyrus and in the inferior insula. BOLD deactivation was found in bilateral posterior cingulate regions (cluster #5, Table 1).

In summary, BOLD activation in the ipsilateral mesial temporal structures, that is, in the presumed epileptogenic focus, and in ipsilateral subcortical structures are seen only 3 s after the TL spikes. Activations in the ipsilateral superior temporal gyrus (i.e., in the presumed generator of TL spikes seen on scalp EEG) and in the ipsilateral inferior insula were found for HRFs peaking 3 and 5 s after the spikes, whereas activations in contralateral areas (superior temporal gyrus and inferior insula) were found only with HRF peaking 5 s after the spike. Posterior cingulate deactivation was found in both peaks.

Discussion

We investigated areas of BOLD changes in a homogeneous population of patients with TLE using an inter-subject group analysis approach. We observed common areas of activation resulting from the TL spikes in the ipsilateral mesial temporal structures, putamen/globus pallidus, as well as bilaterally in the superior temporal gyrus and inferior insula. Deactivation was seen in the bilateral posterior cingulate regions. Because of the small number of patients with different underlying structural abnormalities, we cannot speculate whether there would be subgroups of BOLD pattern, if these individuals could be analyzed as separate groups.

A previous group analysis of nine TLE patients (Laufs et al., 2007) had revealed activation in ipsilateral mesial structures and deactivation in the posterior cingulate gyrus and other regions belonging to the default mode network. Our results, obtained with a larger group of patients and a slightly different statistical approach confirmed the involvement of these structures and demonstrated additional ipsilateral activation in the basal ganglia, insula and superior temporal gyrus. It, therefore, gives evidence of a larger network that is active at the time of TL spikes.

The finding of a consistent activation in the mesial temporal structures as a result of neocortical spikes further supports a dynamic interaction between these two structures at the time of TL spikes. Indeed, the inertia of the hemodynamic phenomena measured with fMRI (few seconds) makes it possible to detect mesial activations at the time of neocortical spikes, even if this mesial BOLD activation was probably caused by a mesial epileptic discharge that cannot be seen on scalp EEG, but that occurred a few milliseconds from the neocortical TL spikes. In the ipsilateral neocortex, we found BOLD activation involving the first temporal convolution for HRFs peaking 3 and 5 s after the spike, and this region is very likely to be the main generator of the TL spikes identified on the scalp EEG. The first temporal convolution is often abnormal and shrunken ipsilaterally to the focus, and this has been observed intraoperatively and by imaging (Earle et al., 1953; Moran et al., 2001).

For the HRF peaking 3 s after the spikes, we found a cluster of BOLD activation involving the ipsilateral hippocampus, the globus pallidus/putamen, and the inferior insula, suggesting

a preferred pathway for propagation of epileptic activity from the mesial structures. Patterns of hypometabolism involving these mesial structures, subcortical structures, and insula were also demonstrated using interictal positron emission tomography (PET) and single photon emission computed tomography (SPECT) studies (Chassoux et al., 2004; Tae et al., 2005).

These regions were activated early and contralateral temporal neocortical activation appeared in the HRF peaking 2 s later. Despite the low temporal resolution of fMRI measurements, one can state with relative confidence that the contralateral activation peaks at least 1 s later than the ipsilateral one. It is interesting to note that this activation is not accompanied by visible EEG changes. It may, therefore, correspond to poorly synchronized neuronal activity. Abnormalities of the superior temporal gyri was also demonstrated through quantitative MRI studies, with significant volume reduction (Moran et al., 2001). The frequent predominance of TL discharges over anterior and inferomedial electrodes would predict that these activations could extend to the temporal pole and inferior temporal region, which we did not observe. However, absence of such responses can be explained by the susceptibility artifact that results in fMRI signal loss in these regions (Ojemann et al., 1997).

It is also noteworthy that the contralateral mesial structures do not show any response (none was significant and none was apparent even when we lowered the significance threshold by excluding the spatial extent threshold, data not shown). The contralateral neocortical activation is, therefore, most likely the result of input from ipsilateral neocortex, rather than from contralateral mesial structures.

Posterior cingulate BOLD deactivation might be due to its involvement in the limbic system, in which the hippocampus plays a central role. The posterior cingulate regions are part of the so-called “default mode network,” which also include the precuneus, and frontal and parietal cortices bilaterally, as highlighted by Raichle et al. (2001). We and others had already observed deactivation involving the “default mode” areas for TL spikes as well as for discharges in other regions (Kobayashi et al., 2006b) The fact that these regions did not appear in this group analysis suggests that although they might be present in individual patients, they are not a common finding across subjects as selected here.

BOLD deactivation at the time of spike and wave discharges in idiopathic generalized epilepsy was clearly demonstrated (Archer et al., 2003; Gotman et al., 2005), and this suspension of the default mode network usually more “active” at rest may partly explain the reduced responsiveness observed in patients with spike and wave discharges (Aarts et al., 1984). Our results suggest that possibly similar phenomena may occur at the time of TL spike, also probably at a lower level of intensity.

Conclusion

We found unilateral involvement of the mesial temporal structures ipsilaterally to the spikes, despite the context of a BOLD signal pattern involving several regions bilaterally. This could be explained by the less extensive connectivity between mesial structures than between neocortical structures (Gloor et al., 1993) and also by the fact that we are studying spikes

most likely having their primary generator in the neocortex. One can, therefore, expect primarily the involvement of regions directly connected to the temporal neocortex.

Whereas spike-related EEG–fMRI has been used primarily in individual patients, it may prove more informative to assess groups of homogeneous patients. We demonstrated a common pattern of BOLD responses at the time of TL spikes, involving mesial temporal structures ipsilateral to the focus, a strong contralateral temporal neocortical component, as well as extratemporal regions. The posterior cingulate deactivation could correspond to the extension of the hemodynamic changes to the limbic system, or to the partial effect of the spikes in the areas related to the default mode network.

Supplementary Material

Refer to Web version on PubMed Central for supplementary material.

Acknowledgments

This project was supported by the Canadian Institutes of Health Research (CIHR) grant MOP-38079. EK is supported by the Milken Family Foundation through the Early Career Physician Scientist Award from the American Epilepsy Society and by the Fonds de Recherche en Santé du Québec (FRSQ). CG is supported by the FRSQ and the Natural Sciences and Engineering Research Council of Canada (NSERC). LT receives a scholarship from the Savoy Foundation for Epilepsy.

References

Aarts JHP, Binnie CD, Smit AM, Wilkins AJ. Selective cognitive impairment during focal and generalized epileptiform EEG activity. Brain. 1984; 107:293–308. [PubMed: 6421454]

Archer JS, Abbott DF, Waites AB, Jackson GD. fMRI ‘deactivation’ of the posterior cingulate during generalized spike and wave. Neuroimage. 2003; 20:1915–1922. [PubMed: 14683697]

Bagshaw AP, Aghakhani Y, Benar CG, Kobayashi E, Hawco C, Dubeau F, Pike GB, Gotman J. EEG-fMRI of focal epileptic spikes: analysis with multiple haemodynamic functions and comparison with gadolinium-enhanced MR angiograms. Hum Brain Mapp. 2004; 22:179–192. [PubMed: 15195285]

Blumenfeld H, McNally KA, Vanderhill SD, Paige AL, Chung R, Davis K, Norden AD, Stokking R, Studholme C, Novotny EJ Jr, Zubal IG, Spencer SS. Positive and negative network correlations in temporal lobe epilepsy. Cereb Cortex. 2004; 14:892–902. [PubMed: 15084494]

Bonilha L, Rorden C, Castellano G, Pereira F, Rio PA, Cendes F, Li LM. Voxel-based morphometry reveals gray matter network atrophy in refractory medial temporal lobe epilepsy. Arch Neurol. 2004; 61:1379–1384. [PubMed: 15364683]

Chassoux F, Semah F, Bouilleret V, Landre E, Devaux B, Turak B, Nataf F, Roux FX. Metabolic changes and electro-clinical patterns in mesio-temporal lobe epilepsy: a correlative study. Brain. 2004; 127(Pt 1):164–174. [PubMed: 14534161]

Collins DL, Neelin P, Peters TM, Evans AC. Automatic 3D inter-subject registration of MR volumetric data in standardized Talairach space. J Comput Assist Tomogr. 1994; 18:192–205. [PubMed: 8126267]

Earle KM, Baldwin M, Penfield W. Incisural sclerosis and temporal lobe seizures produced by hippocampal herniation at birth. AMA Arch Neurol Psychiatry. 1953; 69:27–42. [PubMed: 12996130]

Ebersole JS, Wade PB. Spike voltage topography identifies two types of frontotemporal epileptic foci. Neurology. 1991; 41:1425–1433. [PubMed: 1891092]

Gloor P, Salanova V, Olivier A, Quesney LF. The human dorsal hippocampal commissure: an anatomically identifiable and functional pathway. Brain. 1993; 116:1249–1273. [PubMed: 8221057]

Gotman J, Grova C, Bagshaw A, Kobayashi E, Aghakhani Y, Dubeau F. Generalized epileptic discharges show thalamocortical activation and suspension of the default state of the brain. Proc Natl Acad Sci USA. 2005; 102:15236–15240. [PubMed: 16217042]

Kobayashi E, Bagshaw AP, Benar CG, Aghakhani Y, Andermann F, Dubeau F, Gotman J. Temporal and extratemporal BOLD responses to temporal lobe interictal spikes. Epilepsia. 2006a; 47:1–12.

Kobayashi E, Bagshaw AP, Grova C, Dubeau F, Gotman J. Negative BOLD responses to epileptic spikes. Hum Brain Mapp. 2006b; 27:488–497. [PubMed: 16180210]

Laufs H, Hamandi K, Salek-Haddadi A, Kleinschmidt AK, Duncan JS, Lemieux L. Temporal lobe interictal epileptic discharges affect cerebral activity in 'default mode' brain regions. Hum Brain Mapp. 2007; 28:1023–1032. [PubMed: 17133385]

Lund TE, Madsen KH, Sidaros K, Luo WL, Nichols TE. Non-white noise in fMRI: does modelling have an impact? Neuroimage. 2006; 29:54–66. [PubMed: 16099175]

Merlet I, Gotman J. Reliability of dipole models of epileptic spikes. Clin Neurophysiol. 1999; 110:1013–1028. [PubMed: 10402088]

Moran NF, Lemieux L, Kitchen ND, Fish DR, Shorvon SD. Extra-hippocampal temporal lobe atrophy in temporal lobe epilepsy and mesial temporal sclerosis. Brain. 2001; 124(Pt 1):167–175. [PubMed: 11133796]

Natsume J, Bernasconi N, Andermann F, Bernasconi A. MRI volumetry of the thalamus in temporal, extratemporal, and idiopathic generalized epilepsy. Neurology. 2003; 60:1296–1300. [PubMed: 12707432]

Ojemann JG, Akbudak E, Snyder AZ, McKinstry RC, Raichle ME, Conturo TE. Anatomic localization and quantitative analysis of gradient refocused echo-planar fMRI susceptibility artifacts. Neuroimage. 1997; 6:156–167. [PubMed: 9344820]

Raichle ME, MacLeod AM, Snyder AZ, Powers WJ, Gusnard DA, Shulman GL. A default mode of brain function. Proc Natl Acad Sci USA. 2001; 98:676–682. [PubMed: 11209064]

Ryvlin P, Kahane P. The hidden causes of surgery-resistant temporal lobe epilepsy: extratemporal or temporal plus? Curr Opin Neurol. 2005; 18:125–127. [PubMed: 15791141]

Tae WS, Joo EY, Kim JH, Han SJ, Suh YL, Kim BT, Hong SC, Hong SB. Cerebral perfusion changes in mesial temporal lobe epilepsy: SPM analysis of ictal and interictal SPECT. Neuroimage. 2005; 24:101–110. [PubMed: 15588601]

Thivard L, Lehericy S, Krainik A, Adam C, Dormont D, Chiras J, Baulac M, Dupont S. Diffusion tensor imaging in medial temporal lobe epilepsy with hippocampal sclerosis. Neuroimage. 2005; 28:682–690. [PubMed: 16084113]

Worsley KJ, Liao CH, Aston J, Petre V, Duncan GH, Morales F, Evans AC. A general statistical analysis for fMRI data. Neuroimage. 2002; 15:1–15. [PubMed: 11771969]

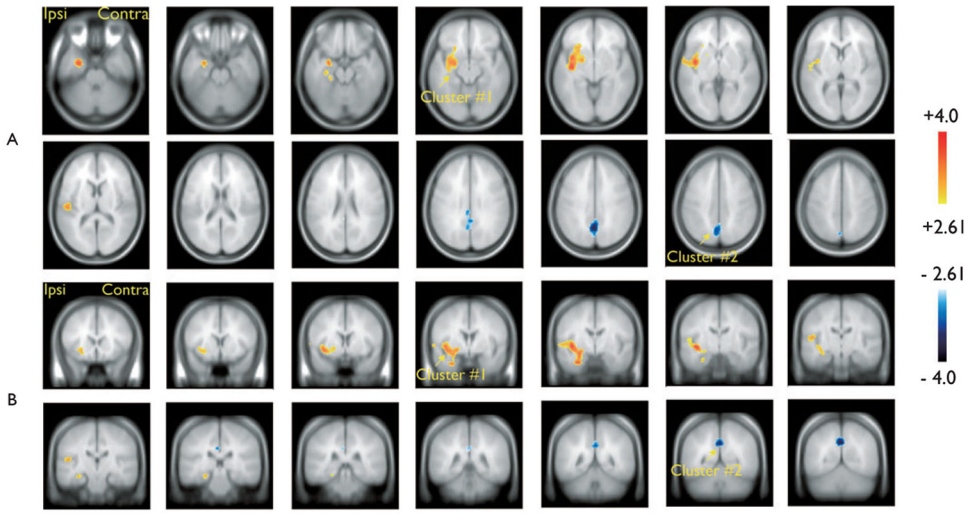

Figure 1.

Group analysis results for the hemodynamic response function (HRF) peaking 3 s after the TL spikes. Resulting t-map ($p < 0.005$ noncorrected) after cluster size test ($p < 0.05$ corrected for spatial extent). (**A**) Sagittal slices (6 mm); (**B**) Coronal slices (6 mm). One cluster of significant blood oxygenation level dependent (BOLD) activation involved ipsilaterally the mesiotemporal structures (including the hippocampus), the putamen/globus pallidus, the inferior insula, and the superior temporal gyrus (cluster #1, Table 1). Significant BOLD deactivation was found in bilateral posterior cingulate regions (cluster #2, Table 1). *Epilepsia* © ILAE

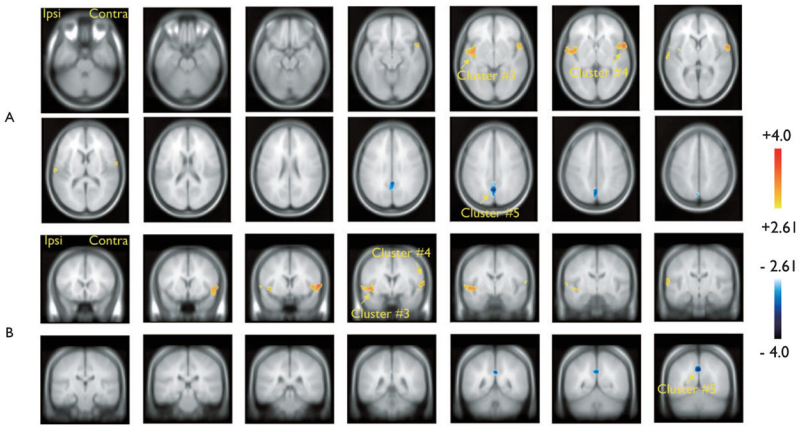

Figure 2.

Group analysis results for the hemodynamic response function (HRF) peaking 5 s after the temporal lobe (TL) spikes. Resulting t-map ($p < 0.005$ noncorrected) after cluster size test ($p < 0.05$ corrected for spatial extent). (**A**) Sagittal slices (6 mm); (**B**) Coronal slices (6 mm). Significant blood oxygenation level dependent (BOLD) activations were found ipsilaterally (cluster #3, Table 1) and contralaterally (cluster #4, Table 1) in the superior temporal gyrus and in the inferior insula. Significant BOLD deactivation was found in bilateral posterior cingulate regions (cluster #5, Table 1).

Table 1

Significant clusters of activation found for the different hemodynamic response functions (HRFs) (corrected $p < 0.05$ for spatial extent). Within each HRF, clusters are ordered by decreasing volume and decreasing level of significance

HRF Peak(s)	Cluster #	Response type	Volume (mm^3)	Spatial extent corrected p-value	Max t-value	Location
3	1	Activation	16,336	0.000	3.88	Ipsilateral mesial temporal, Ipsilateral putamen/globus pallidus Ipsilateral inferior insula Ipsilateral superior temporal
3	2	Deactivation	5,600	0.002	−3.68	Bilateral posterior cingulate
5	3	Activation	4,984	0.003	3.41	Ipsilateral superior temporal Ipsilateral inferior insula
5	4	Activation	4,168	0.010	3.76	Contralateral superior temporal
5	5	Deactivation	3,928	0.013	−3.62	Bilateral posterior cingulate

Epilepsia. Author manuscript; available in PMC 2013 September 10.